Available online at www.sciencedirect.com
ScienceDirect
Journal of the European Ceramic Society 29 (2009) 1561–1569
www.elsevier.com/locate/jeurceramsoc

Microstructural and mechanical changes by chemical ageing of glazed ceramic surfaces

V. Cannillo [a], L. Esposito [b], E. Rambaldi [b], A. Sola [a], A. Tucci [b,*]

[a] *Dipartimento di Ingegneria dei Materiali e dell'Ambiente, Università di Modena e Reggio Emilia, Via Vignolese 905, 41100 Modena, Italy*
[b] *Centro Ceramico Bologna, Via Martelli 26, 40138 Bologna, Italy*

Received 26 June 2008; received in revised form 29 September 2008; accepted 10 October 2008
Available online 18 December 2008

Abstract

In the present work, several ceramic tiles, characterised by different glazes, were considered in order to define the role played by the glassy and crystalline phases on the leaching mechanisms and the deterioration of the mechanical properties. The glazed working surfaces were subjected to chemical attack by using a strong basic solution and the chemical analysis of the leached solutions was performed. Before and after the chemical attack, the glazed surfaces of the samples were analysed from both the microstructural and mechanical point of view. In this context, the microstructure was observed by SEM and analysed by X-ray diffraction. In order to define other possible changes, roughness measurements, Vickers hardness and micro-scratch tests were also performed.

The results made it possible to deepen the understanding of the mechanisms of elements release caused by the chemical attack and their implications on microstructural and mechanical degradation of the working surface of glazed ceramic tiles.

Keywords: Glazed ceramic tile; Alkaline attack; Microstructure; Scratch resistance; Mechanical degradation; Tiles

1. Introduction

Silicatic ceramic surfaces are widely used for heavy duty applications, for both indoor and outdoor destinations. The need to clean the working surface of ceramic tiles with chemical agents, having strongly basic pH, is an usual practice, even if no information is available on the microstructural changes of the working surface and the corresponding decrease in performances. More in general, keeping in mind that tiles interact with the environment they are placed in, it is fundamental to know the capability of their working surface to withstand the different substances they come into contact with. In fact, the chemical resistance of the working surface of glazed ceramic tiles represents an important feature for their quality and correct service life. In this context, a great emphasis is focused on the determination of the chemical resistance, which is reported in the standard EN ISO 10545-13 together with the testing method.[1] However, the standard simply provides a classification based on every effect caused by the contact among the established chemical solutions and the glazed working surface. As a matter of fact, the test results do not give any information about possible damage and mechanical weakening induced in the glaze layer. This occurrence could increase the deterioration rate of the working surface, compromising the life cycle of the tile.

In the literature, several investigations have shown that soda-lime glasses and ceramics are sensitive to humidity.[2–9] Recently, this sensitiveness, in terms of fracture resistance of the working surface of glazed ceramic tiles, to water and chemical solutions has been remarked.[10] The tests, intentionally performed with strong solutions and short times, make it possible to quickly simulate the service conditions, where the working surface of tiles is subjected to frequent washes with the use of cleaning agents whose nature and chemical composition are nearly always unknown. Since, during the life cycle, the working surface of tiles is also exposed to different stresses coming from the environment, if a chemical deterioration occurs, the mechanical resistance is also likely to change. These features, strictly connected with the behaviour of materials and completely ignored in

* Corresponding author. Tel.: +39 051 534015; fax: +39 051 530085.
E-mail address: tucci@cencerbo.it (A. Tucci).

0955-2219/$ – see front matter © 2008 Elsevier Ltd. All rights reserved.
doi:10.1016/j.jeurceramsoc.2008.10.018

the classification of tiles, are going to become very important in view of the current tendency to confer different functionalities to the working surface,[11] due to the requirements to safeguard the characteristics, the reliability and a correct behaviour during service. To acquire such information, a viable testing method could be the determination of the mechanical characteristics, before and after leaching, and the chemical analysis of the leached solutions, to evaluate the presence of the elements given off by the glazed tiles. This method takes into consideration the role played by the microstructure and content in glassy and crystalline phases on the leaching mechanisms and the deterioration of the mechanical characteristics of the glaze layers.

In the present work, addressed to investigate the above-mentioned problems, different glazed ceramic tiles were considered. Microstructural and mechanical characterisation of their working surface was performed before and after a chemical attack by a strong basic solution.[12] To define the role of the glassy and crystalline phases, the results were evaluated also in the light of the chemical analysis of the leached solutions. These determinations contributed, on one hand, to explain the mechanisms of the elements release by the glazed surfaces and, on the other, to evaluate the amount of the degradation of the working surface.

2. Materials and experimental

For the present investigation five different kinds of glazed tiles, single-fired products of 10 cm × 10 cm in dimension, were chosen and denoted as G1, G2, G3, G4 and G5.

The products were characterised by the same ceramic body, the starting composition of which contained 38 wt% of illitic-kaolinitic clays, 49 wt% of feldspars and 13% of silica sand. These raw materials were wet milled and the resulting spray dried powder were uniaxially pressed, at 32 MPa, to obtain 10 cm × 10 cm tiles. The surfaces of all the samples were covered by an intermediate layer of whitish engobe and, subsequently, by different glazes; the double disc technique was used for both the applications. In Table 1, the raw materials used for the preparation of the engobe and glazes are reported. For the different glazes their chemical composition is reported in Table 2.

All the glazed tiles were fired in an industrial roller kiln, with a thermal cycle of 32 min (cold to cold) and maximum temperature of 1170 °C. Their water absorption and the flexural strength values were determined by following the methods recommended respectively in the standard ISO 10545-3 and ISO 10545-4.[13,14] On the basis of the results reported in Table 1 and of the method of manufacture (dry pressing), the studied products are classified as belonging to the group BII_a, according to the standard EN 14411.[15]

In order to establish the critical parameters for the experimental tests, the glaze thickness of all the products was determined on the polished cross section of the samples, by using a metallographic microscope (Leica, DM/LP, D) equipped with an image analyser system (Qwin v.2.2, Leica, D).

The mineralogical phase composition of the glaze layers was assessed by X-ray diffraction analysis (PW3830, Philips, NL), carried out directly on the glaze surfaces, working in a 2θ range of 10–70° with a scanning rate of 0.02° 2θ/s. Even if it was not possible to carry out a quantitative analysis of the phase composition, the qualitative comparison of the relative intensity of the peaks, in the XRD spectra, make it possible to evaluate the level of crystallinity in the different glazes, thanks to the fact that all the tested specimens had the same geometry and were analysed in the same conditions.

Table 2
Chemical analysis of the tested glazes, wt%.

	G1	G2	G3	G4	G5
SiO_2	44.32	48.21	46.09	47.41	66.61
Al_2O_3	11.83	12.89	13.03	13.30	6.28
TiO_2	0.00	0.06	0.27	0.00	0.27
K_2O	2.12	2.04	2.55	1.95	1.83
CaO	2.16	3.09	2.40	4.45	3.11
Fe_2O_3	0.00	0.00	0.00	1.40	0.46
MgO	2.29	0.87	2.37	0.00	0.41
Na_2O	3.42	4.60	2.97	4.53	5.40
ZrO_2	15.35	9.79	11.85	0.67	0.00
ZnO	4.82	5.66	5.37	9.31	5.53
PbO	8.88	6.99	6.68	7.93	4.11
BaO	4.81	5.63	6.42	6.74	5.23
CoO	0.00	0.00	0.00	0.58	0.00
SeO_2	0.00	0.18	0.00	0.00	0.12
CdO	0.00	0.00	0.00	0.00	0.65
Cr_2O_3	0.00	0.00	0.00	1.73	0.00

Table 1
Main characteristics of the tested samples.

Sample	Raw materials, wt%				Glaze thickness, μm	Glazed tile	
	Engobe		Glaze			W.A., wt%	σ, MPa
	Frit*	Crystals**	Frits***	Crystals**			
G1	15	85	75 (a, b)	25	170	5.2	35.5
G2	15	85	76 (a, b, c)	24	171	5.6	36.3
G3	15	85	60 (a, b, d)	40	186	5.6	37.2
G4	15	85	68 (a, b)	32	171	5.8	34.2
G5	15	85	100 (b, c, d)	0	100	5.5	33.7

* Ba, Na based frit.
** Clays, feldspars, quartz, zircon.
*** (a) Ba, Ca, Zn crystallizing frit, (b) Pb based frit; (c) Se based frit; (d) Ba based frit.

The alkaline attack was performed by exposing the glazed surface of the tiles to a KOH solution, 20 g/l, at a constant temperature of 23 °C, for seven days. The chemical analysis of the leached solutions was performed by an atomic emission spectroscopy (Perkin Elmer, ICP-OES Optima 3200 XL, NL), as described elsewhere.[16]

The surface morphology of the as-received and the leached tiles was observed by using a scanning electron microscope (SEM, Zeiss EVO 40, D) equipped with an energy-dispersive X-ray analyser (EDS, Inca, Oxford Instruments, UK). The same system was used also to determine the quantitative chemical composition of the glazes and of selected area, corresponding to the amorphous phases. The chemical compositions values, reported in Tables 2 and 3, are the average of almost five analyses performed in different area and corrected with inner standards.

The average and maximum surface roughness, R_a and R_{max}, were measured on both the as-received and leached surfaces, by using a roughness meter (Hommel Tester, T2000, D), according to the test method recommended in the standard EN 623-4.[17]

Table 3
Chemical analysis of the amorphous phase of the tested glazes, wt%.

	G1	G2	G3	G4	G5
SiO_2	53.33	51.66	52.74	51.46	66.61
Al_2O_3	12.89	12.90	13.37	12.08	6.28
TiO_2	0.00	0.00	0.00	0.00	0.27
K_2O	3.24	2.77	3.43	1.98	1.83
CaO	2.26	4.05	2.63	4.86	3.11
Fe_2O_3	0.00	0.00	0.00	0.36	0.46
MgO	2.10	1.07	2.42	0.30	0.41
Na_2O	3.86	4.77	4.21	5.70	5.40
ZrO_2	0.00	1.51	1.69	0.00	0.00
ZnO	5.24	6.77	5.35	8.10	5.53
PbO	10.57	8.54	7.43	9.37	4.11
BaO	6.51	5.95	6.02	5.38	5.23
CoO	0.00	0.00	0.00	0.21	0.00
SeO_2	0.00	0.00	0.00	0.00	0.12
CdO	0.00	0.00	0.00	0.00	0.65
Cr_2O_3	0.00	0.00	0.00	0.20	0.00

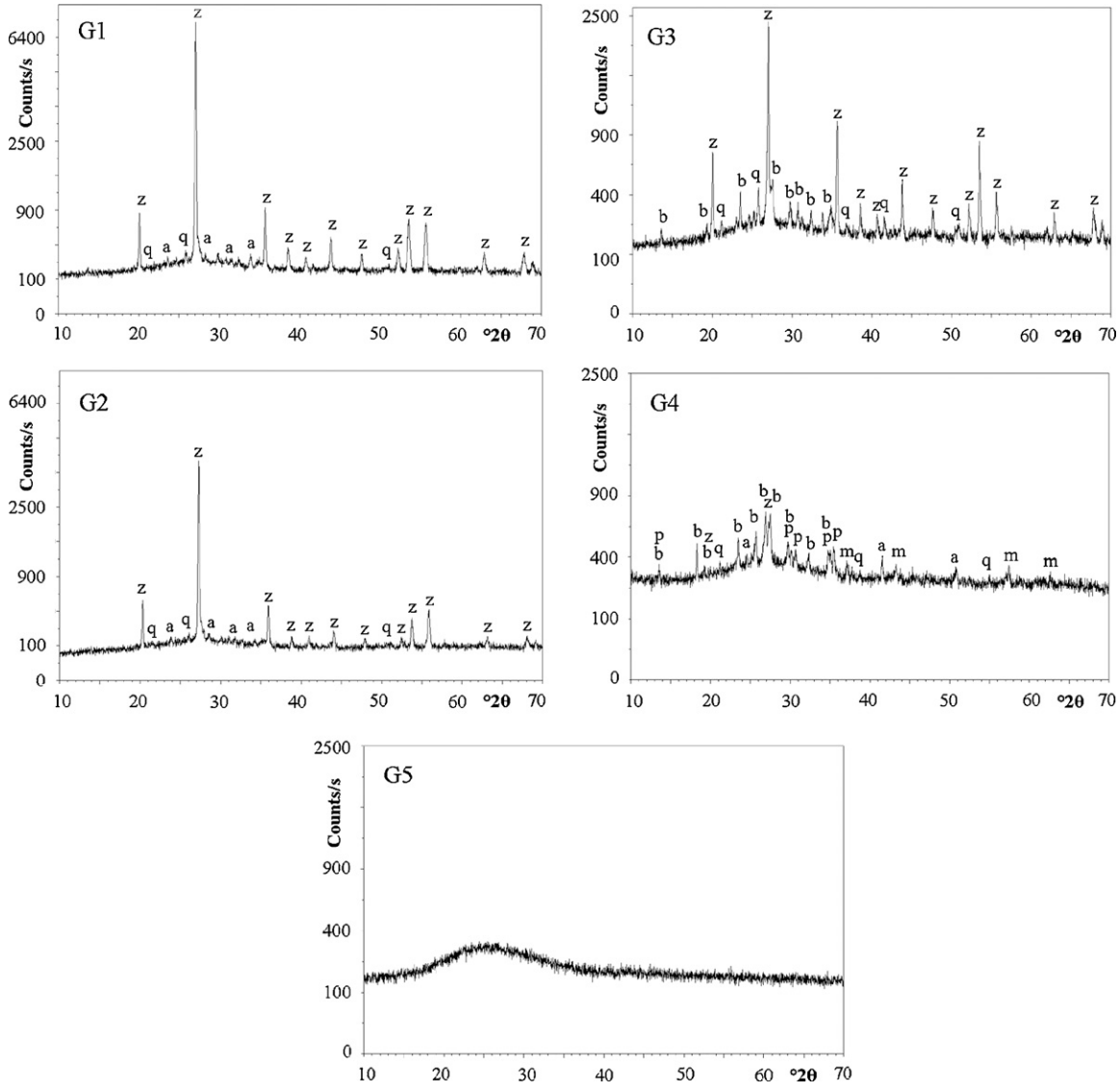

Fig. 1. X-ray diffraction patterns of the G1, G2, G3, G4 and G5 glazes (a = plagioclase, b = celsian, m = magnetite, p = petedunnite, q = quartz, z = zircon).

To detect possible variations of the mechanical performances induced by the chemical attack, hardness and scratch resistance of the glazed surfaces were also determined. Vickers hardness measurements were performed by using a semiautomatic hardness tester (Zwick 3212, D), applying an indentation load of 0.5 N and micro-scratches were produced on the surfaces of suitable specimens (∼10 mm × 20 mm) with the aid of a specific instrument (Scratch Tester, Open Platform, CSM Instruments SA, CH). The tests were performed by using a Rockwell diamond tip, 200 μm in diameter, which was drawn across the glazed surface under a progressively increasing load ("progressive scratch"). The following conditions were used: initial load of 1 N, final load of 30 N, loading rate of 14.5 N/min and scratch length of 2 mm (corresponding to an indenter tip speed of 1 mm/min). The instrument is also equipped to detect the acoustic emission, as well as the normal load applied to the glazed surface, the tangential and friction force. The scratch tracks, three for each samples, were observed by an optical microscope and SEM to identify the critical load[18] and to evaluate the possible mechanical degradation of the glazed surfaces caused by the chemical attack. In order to define the influence of the glaze composition on the scratch resistance, soda-lime

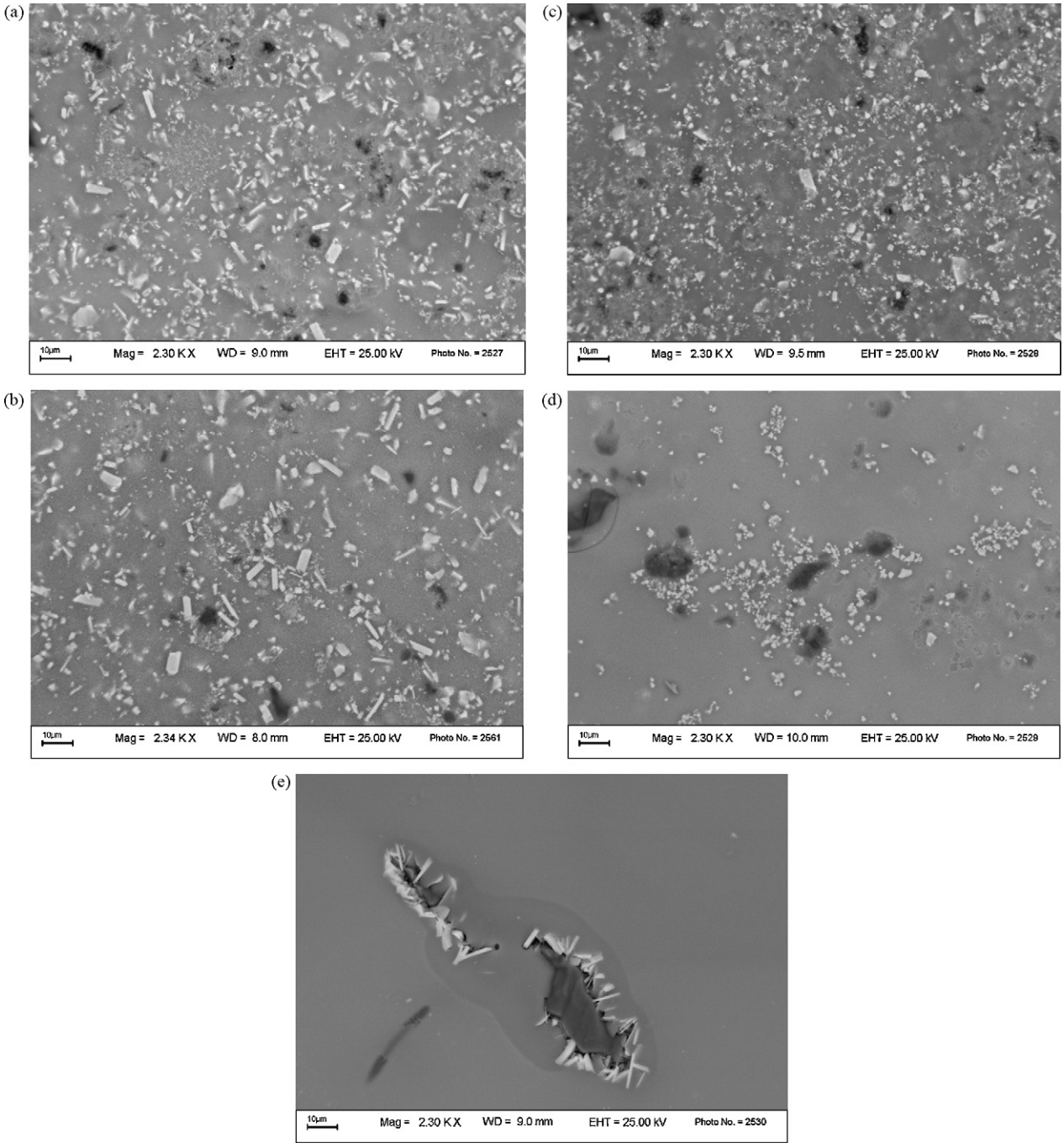

Fig. 2. SEM–BEI micrographs of the surface of samples: (a) G1, (b) G2, (c) G3, (d) G4 and (e) G5 (after chemical attack).

glass samples were also tested, considering them as a reference material.

3. Results and discussion

The comparison of the XRD spectra, collected on the glaze layer of all the tested samples (Fig. 1), shows that the amount of glassy phase progressively increases from sample G1 to sample G5. In particular, as regards G1 and G2, the glaze presents a rather low amount of glassy phase and zircon is the main crystalline phase with a small amount of plagioclase and quartz. The different colour of the glazes, G1 yellow and G2 orange, has to be attributed to the higher amount of zircon, a white pigment, in G1. Zircon is present also in G3, white glaze, associated with alkaline feldspars and quartz, but in a rather higher amount of glassy matrix. The SEM observation of the surfaces of G1, G2 and G3 shows that the zircon crystals (Fig. 2 a–c) are homogeneously distributed in the glassy phase and they are characterised by a well evident plate-like shape, while quartz and feldspar (plagioclase and celsian) crystals (black spots in Fig. 2 a–c) do not present well defined grain boundaries, evidence of a partial reaction with the surrounding glassy phase.

The degree of crystallization of G5 sample, red colour, is so low that the XRD analysis (Fig. 1) does not detect the presence of any crystalline phase, even if, from SEM observation, traces of small alumina grains surrounded by elongated calcium aluminate crystals can be observed (Fig. 2e). Similarly, in G4 sample, black colour, even if the degree of crystallization is low, small peaks, corresponding to a calcium-zinc silicate (petedunnite), celsian, magnetite, plagioclase, zircon and quartz (Fig. 1), are present. While petedunnite and magnetite are used as pigments, zircon, plagioclase and quartz are relict of unmelted raw materials and celsian crystals are new phases derived from the barium-based crystallizing frits. As revealed in sample G5, the location of the calcium aluminate crystals suggests that they are new crystals formed during sintering at the boundary between the alumina grains and the melted glass. These newly formed crystals are small in size, less than 5 μm, and they are mainly grouped in very defined areas, where the crystallization conditions were satisfied during the firing step. This causes some microstructural non homogeneities.

The results of the leaching tests of the tested samples are reported in Table 4. To clarify the different behaviours presented by the tested samples, it is necessary to underline, that, as reported from the literature,[19] the contact of a silicate glass with a water-based solution causes ion exchange phenomena, with a preferential extraction of alkali ions. In this way, an alkali modified surface film, rich in silica, is formed on the glass surface; the thickness and mechanical characteristics of such a film depend on both the chemical composition of the glass and the test conditions, i.e. time, pH and temperature. Although, silicate glasses are generally resistant to water and acid attack, they are susceptible to strong alkaline solutions, because OH^- ions are able to attack the silica-rich layer by breaking the silica–oxygen link, thus decomposing and dissolving the silicate network.[20] According to this mechanism, in the leached solutions, Table 4, while the amount of elements, such as aluminium, calcium, magnesium, zinc, lead and barium, is rather low and substantially the same for all the samples; the leaching of silicon and sodium is much higher and their relative amount is quite different for different samples. Such behaviour can be related with the amount and chemical composition of the glassy matrix of the tested glazes. From Table 4, the silicon and sodium release is different, even though the original contents in the amorphous phase of the unleached samples are not significantly different (Tables 2 and 3). In particular, the silicon and sodium percentages are lower for those samples characterised by a high crystalline phase content. In fact, G1 and G2, which are highly crystalline glazes, show a very low release of silicon and sodium (the contents in the leached solutions are respectively 1.47 and 0.33wt% for G1, and 1.36 and 0.40wt% for G2), while the silicon and sodium contents rise to 2.16 and 3.10wt% for G3 and 3.32 and 3.73wt% for G4, which are less crystalline. As listed in Table 4, the sample G5, which is almost completely amorphous, shows a relatively low loss of silicon and sodium, lower – for example – than sample G4, which is more crystalline; the reason has to be attributed to the chemical composition of the G5 (Table 2), that, compared to the other samples (Table 4), contains the minimum amount of modifying oxides, such as PbO. Due to its molecular dimensions, such kind of oxide strongly destabilize the network structure of glasses, decreasing their chemical durability, more than BaO, CaO and NaO.[21]

Table 4
Chemical analysis of the leached solutions after alkaline attack, wt%.

	G1	G2	G3	G4	G5
Si	1.47	1.36	2.16	3.32	2.40
Al	0.02	0.10	0.00	0.00	0.00
Ca	0.01	0.00	0.01	0.00	0.00
Mg	0.03	0.02	0.03	0.02	0.01
Na	0.33	0.40	3.10	3.73	1.68
Zn	0.01	0.05	0.04	0.03	0.02
Pb	0.07	0.07	0.16	0.10	0.03
Ba	0.03	0.02	0.00	0.02	0.03

The morphological study of the corroded surfaces confirms as, for all the samples, the glaze corrosion starts from the depolymerising of the glassy phase (Fig. 3a). Such reacted layer, characterised by a reduced density,[19] successively detaches revealing rather smooth areas of bulk glass (Fig. 3b), where residual crystals may survive thanks to their higher resistance to the basic chemical attack (Fig. 3c).

The surface of the most crystalline sample, G1, evidences a large presence of crystal structures, whose boundaries have been highlighted by the dissolution of the glassy phase (Fig. 3c). The surface of sample G5, which is almost completely amorphous, results to be the most homogeneous and smooth one after chemical attack (Fig. 4a), even if the few crystals of alumina and the fine acicular crystals of calcium aluminate, which are present in the glassy matrix as mentioned above, have been revealed (Figs. 2a and 4b).

Since the chemical attack did not affect the crystalline phases, after leaching the most crystalline glazes showed a greater amount of crystal grains than the most amorphous ones. As a consequence, the unevenness of the surface morphology is more

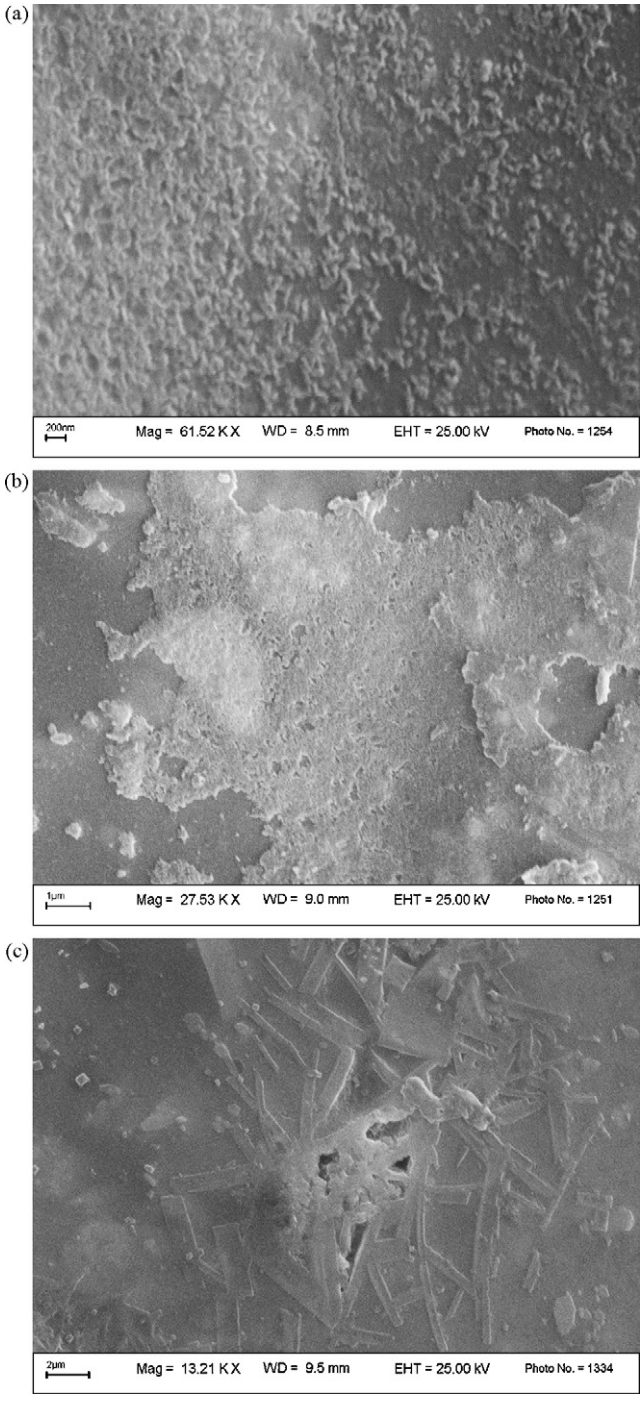

Fig. 3. SEM–SEI micrographs of the surface, after chemical attack with KOH of samples: (a) and (b) G3 and (c) G1.

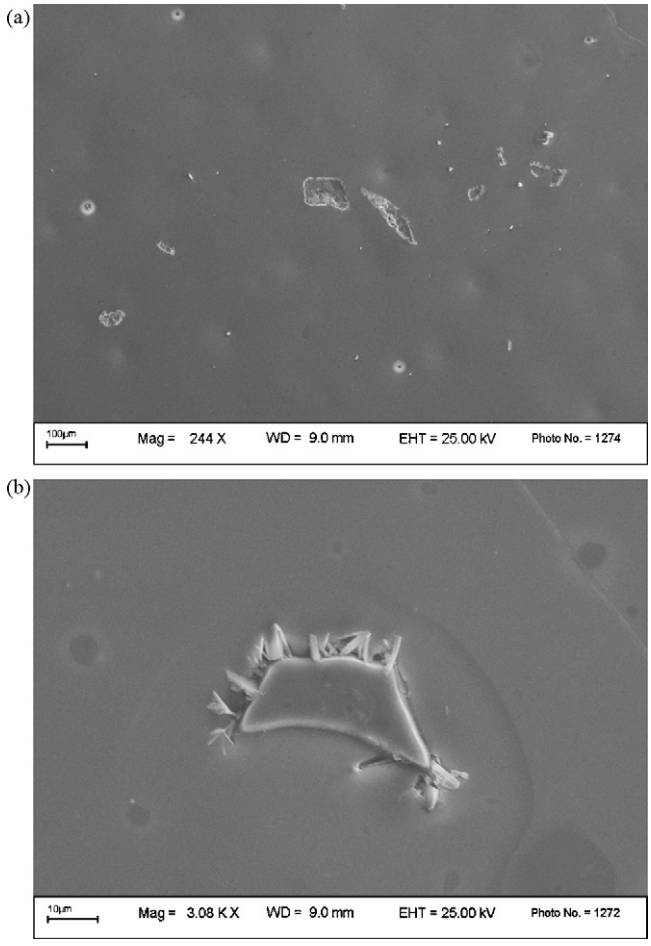

Fig. 4. SEM micrographs of the surface after chemical attack with KOH of G5 samples: (a) G5 and (b) G1.

relevant in the highly crystalline samples than in the amorphous ones, as confirmed by the results of the roughness tests (Table 5). In fact, R_a values are usually increased by the alkaline attack, but this phenomenon is especially evident in the highly crystalline glazes, whose roughness resulted so high, that the measure could not be performed. The same trend was confirmed also by the maximum roughness values, R_{max}.

As shown in Table 5, in spite of the different crystallinity exhibited by the glazes, the Vickers hardness values of the different samples are included in a rather narrow range, probably due to the large amount of silicate glassy matrix which characterises all these kinds of glaze layers. After the alkaline attack, the hardness significantly decreases only for samples G4 and

Table 5
Vickers hardness HV (0.5 N) and average and maximum roughness, R_a and, R_{max}, of the tested glazes, before and after alkaline attack.

	HV, GPa		R_a, µm		R_{max}, µm	
Sample		Etched		Etched		Etched
G1	7.2 ± 0.7	7.4 ± 0.5	0.94 ± 0.12	nd	7.18 ± 2.18	nd
G2	7.4 ± 0.7	7.2 ± 0.5	0.87 ± 0.05	nd	7.21 ± 2.19	nd
G3	7.3 ± 0.8	nd	0.67 ± 0.05	0.72 ± 0.08	5.30 ± 0.52	6.32 ± 0.92
G4	6.9 ± 0.7	6.0 ± 0.5	0.51 ± 0.08	0.65 ± 0.06	5.05 ± 0.97	5.19 ± 1.49
G5	7.3 ± 0.6	6.5 ± 0.2	0.70 ± 0.09	0.70 ± 0.15	4.96 ± 1.45	5.14 ± 1.44

Table 6
Scratch critical load Lc of the tested glazes before and after alkaline attack.

Sample	Lc, N	
		Etched
G1	15.5	15.5
G2	14.1	14.1
G3	12.8	9.5
G4	14.0	13.0
G5	8.6	4.7
SL glass	5.6	10.1

G5, the ones characterised by the heaviest corrosion. It can be deduced that a high content of crystalline phases, limiting the chemical attack, also prevents the decrease in surface hardness. As regards the sample G3, it was not possible to measure its hardness after the chemical attack, because the excessive surface deterioration made it impossible to clearly measure the impression dimensions.

The scratch resistance of the different glazes, before and after the alkaline attack, can be assessed by the analysis of the critical load values, Lc.[22] In the present work, it was assumed that the critical load corresponds to the appearance of the first complete circular ring crack. The values, determined by means of SEM observation, are reported in Table 6.

The as-received soda-lime glass, considered as reference material, is characterised by the lowest Lc value. However it is worth noting that, after alkaline attack, the soda-lime glass presented an anomalous behaviour, since the Lc value was higher than that measured for the as-received surface. This increase in scratch resistance (i.e. increase in Lc) can be related to the large amount of sodium ions that are easily exchanged with the potassium ones which are present in the alkaline solution.[23] The larger dimension of the potassium ions causes an expansion of the soda-lime glass network of the sub-surface layer, constrained by the bulk material below. As a consequence, a surface layer, about 100 μm in thickness, is subjected to a compression stress field. This surface condition could be able to enhance the scratch resistance. The cracks arise and develop, following the same evolution observed on the surface of the as-received soda-lime glass, only when the stress field induced by the applied load overcomes the compressive stress field.

As regards the glaze layers, it should be noted that during each scratch test, due to the progressive increase of the applied load, the penetration depth of the indenter tip increases, reaching its maximum at the end of the scratch. The maximum depth, especially after chemical attack, can be as high as 60–70 μm, a value which is lower than the glaze layer thicknesses (Table 1). That does not invalidate the Lc evaluation, since the indenter tip is very far from the ceramic substrate when the Lc is reached. In fact, as shown in Table 6, Lc is at most 15.5 N. Moreover,

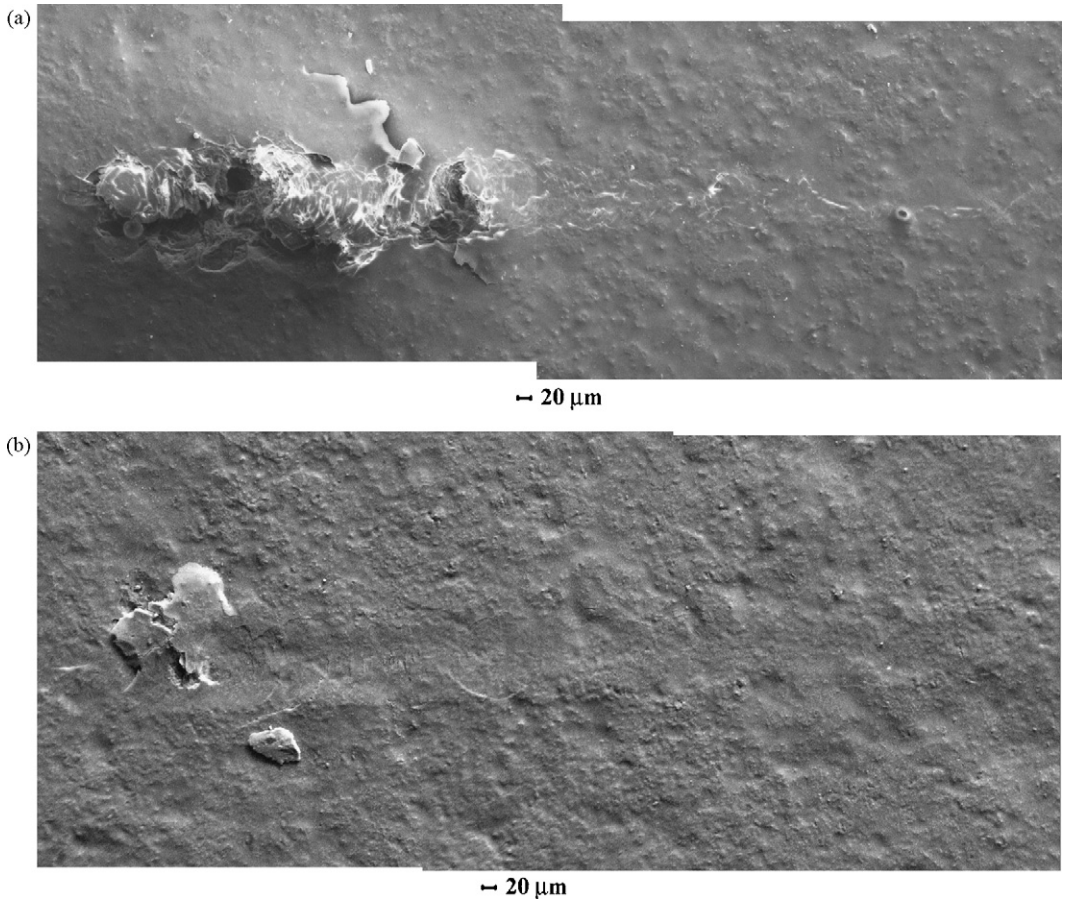

Fig. 5. SEM micrographs of representative scratches: samples (a) G4 and (b) G1.

the ceramic substrate is the same for all the samples, hence the differences in the glaze behaviour are to be ascribed only to the intrinsic properties of the glaze layer.

The G5 glaze, even if it is almost completely amorphous, presents a Lc value rather higher than the soda-lime glass. Such difference depends essentially on the development of a compression stress field in the glaze layer of G5, during the firing step, caused by the different expansion coefficient between the ceramic body and the glaze layer, not present in the soda-lime glass, that prevents the crazing phenomena.[20]

As a general trend, the presence of crystalline phases contributes to increase the Lc in the as-received samples, Table 6. For example, G4, just slightly more crystalline than G5, reveals a higher scratch resistance (i.e. higher value of Lc). Moreover, after the chemical attack, the poorly crystalline samples, characterised by a higher leaching effect, showed a remarkable decrease in Lc. G1 and G2, the more resistant ones from a chemical point of view, present rather similar Lc values before and after the alkaline attack. As a matter of fact, the SEM observation of these samples, before and after chemical attack, reveals only light morphological changes, which do not seem to affect their mechanical behaviour.

Additional information may derive from the analysis of the scratch morphology, which is particularly significant for sample G4. In fact, even if it contains a low amount of crystalline phases, the Lc measured is rather similar to that of the more crystalline ones; however, the analysis of the scratch morphology reveals

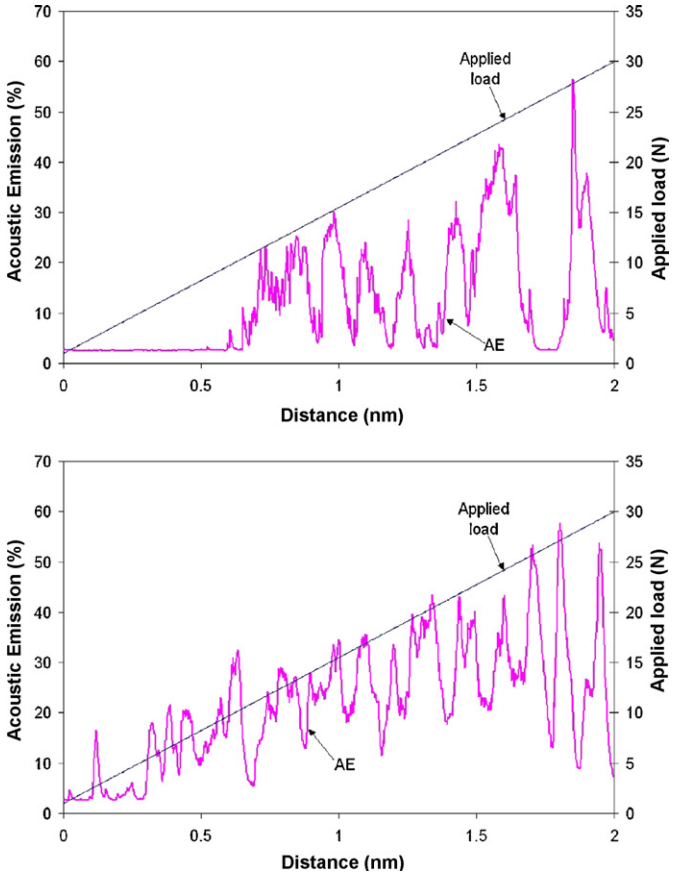

Fig. 6. Acoustic emission curve: samples (a) G5 and (b) G1.

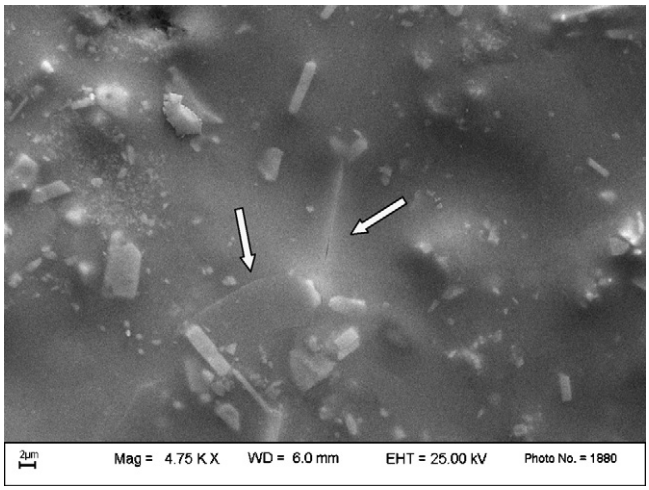

Fig. 7. SEM micrograph of the surface of sample G1, near the first contact zone indenter-surface: the arrows point out the development of cracks.

that the lateral damaged areas, around the scratches, are much more extended than in the highly crystalline samples (Fig. 5). The material removal mode drastically changes, as observed also in other class of ceramics,[24,25] revealing a transition to a prevailing brittle behaviour.

The effect of the surface roughness on the crack propagation modes may be appreciated by the acoustic emission evaluation. In fact, for very smooth surfaces, which are strictly related to the presence of a large amount of glassy phase, it becomes rather clear that the acoustic emission is very low at the beginning of the scratch test; then it suddenly increases when the first ring cracks form. This is the case, for example, of the soda-lime glass and sample G5 (Fig. 6a). As regards the rough surface of highly crystalline samples, small cracks immediately form at the first contact between the surface asperities and the indenter tip (Fig. 7). Such small cracks do not compromise the functionality of the glaze layer, however the crack initiation is revealed by the presence of several peaks of the acoustic emission. This behaviour is typical of highly crystalline samples, such as G1 (Fig. 6b). As a matter of fact, for every crystalline sample it is extremely difficult to identify the Lc on the basis of the acoustic emission and only microscopic observations can be sound.

4. Conclusions

In the present research, in order to investigate the effect of a chemical ageing which simulates the action of cleaning products and other chemicals in the environment, different glazed single-fired tiles were subjected to a strong alkaline attack and characterised from a chemical, microstructural and mechanical point of view.

The different content in crystalline phases deeply influenced the behaviour during the chemical ageing, since the alkaline attack selectively affected the silicate glass matrix, leaving the crystals almost unaltered. As a consequence, not only the highly crystalline glazes showed superior mechanical properties than the glassy ones, but also resisted the chemical attack better. In fact, after the chemical ageing, the decrease in Vickers hardness

and scratch resistance was more relevant for the amorphous glazes than for the highly crystalline ones.

As regards the scratch resistance, the combined analysis of surface morphology and acoustic emission proved different mechanisms, depending on the glaze crystallinity: poorly crystalline glazes underwent a wide superficial depolymerisation and material removal, which resulted in smooth, but mechanically weakened surfaces, characterised by the development of well defined ring cracks under low applied loads; highly crystalline glazes exhibited a very rough surface, due to the surviving crystals brought to light by the selective removal of the silicate glass matrix, and the first contact of the scratching tip with the surface asperities immediately caused small cracks – perceived by the acoustic emission recording – without compromising the glaze functionality, while the real critical load – defined by SEM – was significantly higher. Aside the content in crystalline phases, the relevance of the chemical composition was revealed by the analysis of the scratch tests on a bulk soda-lime glass (reference material), whose resistance was increased (and not reduced) by the chemical ageing, since the exposure to the KOH solution promoted a Na-K ion exchange, producing a compressive stress in the sub-surface layer, which improved the glass strength.

References

1. EN ISO 10545-13, Ceramic tiles Part-13. Determination of chemical resistance, 2000.
2. Wierderhorn, S. M., Influence of water vapour on crack propagation in soda-lime glass. *J. Am. Ceram. Soc.*, 1967, **50**, 407–414.
3. Yoda, M., Subcritical crack growth in soda-lime glass under combined modes I and III loading. *J. Am. Ceram. Soc.*, 1990, **73**, 2124–2127.
4. Michalske, T. A. and Freiman, S. W., A molecular mechanism for stress corrosion in vitreous silica. *J. Am. Ceram. Soc.*, 1983, **66**, 284–288.
5. Freiman, S. W., McKinney, K. R. and Smith, H. L., Slow crack growth in polycrystalline ceramics. In *Fracture Mechanics of Ceramics*, ed. R. C. Bradt, D. P. H. Hasselman and F. F. Lange. Plenum Press, NY, 1974, pp. 659–676.
6. Bansal, G. K. and Duckworth, W. H., Effects of moisture-assisted slow crack growth on ceramic strength. *J. Mat. Sci.*, 1978, **13**, 239–242.
7. Wachtman, J. B., Subcritical crack propagation. *Mechanical Properties of Ceramics*. John Wiley & Sons, Inc., NY, 1996, pp. 117–140.
8. Wiederhorn, S. M., Subcritical crack growth in ceramics. In *Fracture Mechanics of Ceramics*, ed. R. Bradt, D. P. H. Hasselman and F. F. Lange. Plenum Press, NY, 1974, pp. 613–646.
9. Alban, C., Esposito, L., Rambaldi, E. and Tucci, A., Post-indentation slow crack growth in vitreous mosaic tesserae. In *Proceedings of QUALICER 2008, vol. 2*, 2008, pp. P.BC 75–P.BC 84.
10. Esposito, L., Naldi, D., Rambaldi, E. and Tucci, A., Slow crack growth (SCG) in glazed ceramic tiles. In *10th European Ceramic Society Conference*, 2007.
11. Moreno, A., Ceramic tiles: above and beyond traditional applications. *Bol. Soc. Esp. Ceram. V.*, 2006, **45**(2), 59–64.
12. Karasu, B. and Cable, M., The chemical durability of SrO-MgO-ZrO_2-SiO_2 glasses in strongly alkaline environments. *J. Eur. Ceram. Soc.*, 2000, **20**, 2499–2508.
13. EN ISO 10545-3, Ceramic tiles. Part 3. Determination of Water Absorption, Apparent Porosity, Apparent Relative Density and Bulk Density, 1995.
14. EN ISO 10545-4, Ceramic tiles. Part 4. Determination of Modulus of Rupture and Breaking Strength, 1995.
15. European Standard EN 14411, Ceramic Tile—Definitions, Classification, Characteristics and Marking, 2003.
16. Esposito, L., Rambaldi, E., Tucci, A., Bonvicini, G., Albertazzi, A. and Timellini, G., Chemical ageing andmicrostructural changes of glazed ceramic tile surfaces. *cfi/Ber.DKG*, 2008, **85**(No. 6), E64–E67.
17. European Standard EN 623-4, Advanced technical ceramics-monolithic ceramics-general and textural properties. Part 4. Determination of surface roughness, 1993.
18. ISO 20502, Fine ceramics (advanced ceramics, advanced technical ceramics)—Determination of adhesion of ceramic coatings by scratch testing, 2005.
19. Reinhard, C., Chemical durability of oxide glasses in aqueous solutions: a review. *J. Am. Ceram. Soc.*, 2008, **91**, 728–735.
20. Eppler, R. and Eppler, D., *Glazes and Glass Coatings*. American Ceramic Society, Ohio, 2000.
21. Morey, G. W., *The Properties of Glass*. Reinhold Publishing Corporation, American Ceramic Society, Waverly Press, Baltimore, 1954.
22. International Standard ISO 20502-2005, Fine ceramics (advanced ceramics, advanced technical ceramics)—Determination of adhesion of ceramic coatings by scratch testing.
23. Garza-Méndez, F. J., Hinojosa-Rivera, M., Gómez, I. and Sánchez, E. M., Scaling properties of fracture surfaces on glass strengthened by ionic exchange. *Appl. Surface Sci.*, 2007, **254**, 1471–1474.
24. Subhash, G. and Klecka, M., Ductile to brittle transition depth during single-grit scratching on alumina ceramics. *J. Am. Ceram. Soc.*, 2007, **90**, 3704–3707.
25. Klecka, M. and Subhash, G., Grain size dependence of scratch-induced damage in alumina ceramics. *Wear*, 2008, **265**(5–6), 612–619.